Dalton Transactions

A Reagent for Heteroatom Borylation, Including Iron Mediated Reductive Deoxygenation of Nitrate yielding a Dinitrosyl Complex

Journal:	*Dalton Transactions*
Manuscript ID	DT-ART-01-2020-000077
Article Type:	Paper
Date Submitted by the Author:	08-Jan-2020
Complete List of Authors:	Caulton, Kenneth; Indiana University, Department of Chemistry Beagan, Daniel; Indiana University Bloomington, Department of Chemistry Carta, Veronica; Indiana University

ARTICLE

A Reagent for Heteroatom Borylation, Including Iron Mediated Reductive Deoxygenation of Nitrate yielding a Dinitrosyl Complex

Received 00th January 20xx,
Accepted 00th January 20xx

DOI: 10.1039/x0xx00000x

Daniel M. Beagan, Veronica Carta and Kenneth G. Caulton*

4,4' bipyridyl is shown to be a catalyst for transfer of pinacolboryl groups from $(Bpin)_2$ to nitrogen heterocycles and to Me_3SiN_3. Using stoichiometric $(Bpin)_2$(pyrazine) or $(Bpin)_2$(bipyridine) in an analogous manner, an aromatic nitro group is deoxygenated and subsequently borylated, and four-fold deoxygenation of $(DIM)Fe(NO_3)_2(MeCN)$ to yield the dinitrosyl complex $(DIM)Fe(NO)_2$ is facile. The co-product $O(Bpin)_2$ is the quantitative fate of the removed oxo groups. With borylation of both nitrogen heterocycles and doubly deoxygenating two nitrates coordinated to a single metal center, broad spectrum methodology is demonstrated.

Introduction

Transfer of divalent groups, particularly O and NR hold a fascination because they involve a two electron redox step and because of the limited number of sources of these high energy, six valence electron neutral fragments. We explore here such a transfer, but in the opposite direction: removal of O from a substrate. Strategies addressing this goal in general employ reducing agents which can be collectively called oxophilic: elemental magnesium and silicon or boron compounds.[1-4] Disilane and diboryl compounds certainly have the thermodynamic potential for deoxygenation, but the non-polar character of these element-element bonds is used to explain the kinetic limitations that make them generally unsuccessful in the absence of a catalyst.[5, 6] Our group has recently shown double deoxygenation of a chromium nitrate complex to a chromium nitrosyl using the bis-silyl substituted dihydropyrazine **2** (Scheme 1), which incorporates polar Si-N bonds[7], a motif extensively explored by Mashima for various reductive applications.[8] We explore here extension of early work by Suginome in the use of boryl substituents attached to unusual nitrogen in an eight π electron system which favors boryl transfer by aromatization of the nitrogen heterocycle (Scheme 1).[9]

Ease of preparation makes $(Bpin)_2Pz$ **1** an attractive alternative to **2**, with $(Bpin)_2$ (pin = pinacolate) undergoing a facile reaction with pyrazine to form **1**, without the need of K or Na reductant necessary for the synthesis of **2** from pyrazine and Me_3SiCl.[10] Suginome has shown organocatalytic borylation of substituted pyrazines using $(Bpin)_2$ and catalytic 4,4'-bipyridine, bpy (Scheme 2), as well as stereoselective borylation of electron poor alkynes.[11, 12] We describe here progress on boryl transfer, both stoichiometric and organocatalytic, to sp^2 nitrogen, and also aromatic NO_2 groups, but then move to deoxygenation of nitrate, activated by coordination to

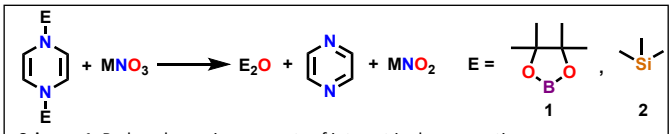

Scheme 1. Reduced pyrazine reagents of interest in deoxygenation

Indiana University, Department of Chemistry, 800 E. Kirkwood Ave., Bloomington, IN, 47401, USA. E-mail: caulton@indiana.edu

†Electronic Supplementary Information (ESI) available: Spectral data, XRD information, computational data. See DOI: 10.1039/x0xx00000x

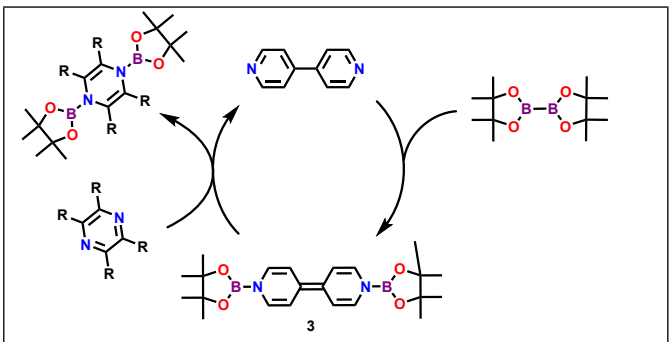

Scheme 2. Organocatalytic borylation of substituted pyrazines using $(Bpin)_2$ and 4,4'-bipyridine reported by Suginome

an iron electrophile, yielding a dinitrosyl iron complex (DNIC), a conversion which is rare, and also relevant to remediation of nitrate pollution, which is the cause of eutrophication of poorly circulating bays and lakes, and the cause of aquatic "dead zones".[13-20] Overall, this report promotes these bis-boryl reagents as potent tools for reductive transformations, pertinent to our goals of nitrogen oxyanion reduction[21-25], as well as broadening the scope and applicability of reduced N-heterocycles.[26]

Results and Discussion

Heteroatom borylation

N=N borylation

We anticipate a mechanistic benefit with **1**, absent in **2,** from the available boron p orbital on the Bpin moieties, which is evidenced in the LUMO + 1 of **1** shown in Figure 1. We expect this π orbital to accept electron density from lone pairs, and thus see **1** as attractive to react with heteroatoms. Importantly, the Lewis acidity of the empty π orbital is *not* quenched by π donation from the pyrazine nitrogen or Bpin oxygens, as shown in LUMO + 1 of this reagent (Fig 1).

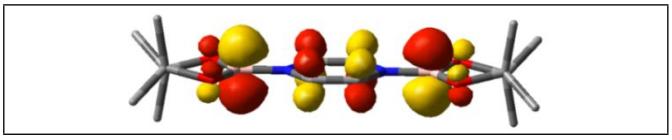

Fig 1. LUMO + 1 (E = +0.2 eV) of geometry-optimized **1** (isovalue 0.05 au)

To this end, we sought to borylate azobenzene; azobenzene is not silylated by **2**. Reaction of equimolar **1** and azobenzene in d_8-toluene shows complete conversion to borylated azobenzene (Scheme 3) in 36 hours at 110 °C. Interestingly, the ^{1}H NMR spectrum (Fig S1) of borylated azobenzene shows two Bpin methyl chemical shifts in a 1:1 intensity, consistent with hindered rotation about the N-B bonds.

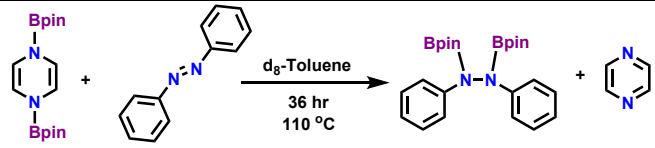

Scheme 3. Borylation of azobenzene using **1**

Azobenzene has previously been borylated catalytically by Braunschweig using a Pd catalyst and $(Bpin)_2$[27], and given Suginome's success using 4,4'-bpy to deliver two BPin fragments to substituted pyrazine, we sought *catalytic* borylation of azobenzene using $(Bpin)_2$ and 4,4'-bpy. With 30 mol % catalyst loading of 4,4'-bpy, azobenzene is cleanly borylated by $(Bpin)_2$ at 110 °C in d_8-toluene in 12 hours, representing the first organocatalytic borylation of an N-N bond using $(Bpin)_2$. A high catalyst loading was chosen to enhance the rate of the reaction, and the 4,4'-bpy catalyst can be recovered from the reaction mixture during purification. The success of **1** in this transformation (in comparison to **2**) corroborates our expectation that **1** has a mechanistic benefit in the form of an empty p orbital on the boron, which most likely accepts electron density from the lone pairs on the nitrogens of azobenzene. In acetonitrile solvent the catalytic reaction proceeds analogously, with clean formation of the borylated azobenzene after 12 hours of heating; however, using excess $(Bpin)_2$, **3** is observed by ^{1}H NMR after the reaction is complete. The borylated bipyridine **3** (Scheme 2) has low solubility in acetonitrile, and X-ray quality crystals form in the reaction mixture. The crystal structure of **3** (Fig 2), shows the two Bpin fragments are coplanar with the reduced bipyridine, consistent with formation of a double bond between C4 and C4'.

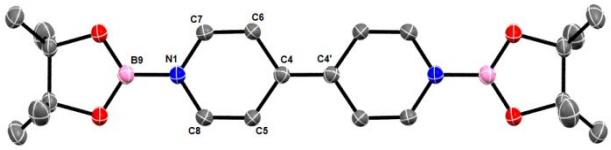

Fig 2. Molecular structure of **3** showing selected atom labelling. Ellipsoids are plotted at the 50% probability level. Hydrogen atoms are omitted for clarity. An inversion center is present on the C4-C4' bond, resulting in half the molecule being the asymmetric unit. Selected structural parameters (Å): N1-C7, 1.399(2); N1-C8, 1.395(3); N1-B9, 1.430(3); C4-C4', 1.375(4); C4-C5, 1.440(3); C4-C6, 1.457(3); C5-C8, 1.329(3); C6-C7, 1.331(3).

We next sought to generalize this catalytic borylation to other N=N double bond fragments. Benzo(c)cinnoline (bcc) can also be catalytically borylated (Scheme 4) in 30 hours in C_6D_6 at 100 °C.

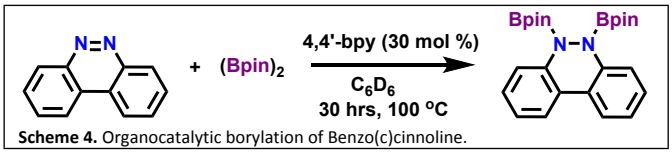

Scheme 4. Organocatalytic borylation of Benzo(c)cinnoline.

We were interested in establishing if there were detectable differences in the borylation *rate* between azobenzene and bcc based on the *trans vs. cis* geometry about their N=N bonds. This was done by an internal competition between azobenzene, bcc, and $(Bpin)_2$ in a 1:1:1 mole ratio with 30 mol % 4,4'-bpy in d_8-toluene at 110 °C. Periodic ^{1}H NMR monitoring (Fig S4) of the reaction progress under these boron-deficient conditions showed a high selectivity for borylation of bcc, with only small amounts of borylated azobenzene formed. Although bcc has a more negative reduction potential (more difficult outer sphere 1e reduction)[28], we rationalize the selectivity for bcc via a mechanistic benefit of having the nitrogen lone pairs *cis*, thus minimizing reorganization energy to reveal the initially *trans* N=N bond in azobenzene.

We were also interested in the borylation of azides to form amines with subsequent loss of N_2; analogous silylation is computed to be highly (-74 kcal/mol) exergonic by **2**, yet does not occur. Reaction of $TMSN_3$ and $(Bpin)_2$ in a 1:1 mole ratio with 30 mol % 4,4'-bpy results in compete consumption of $TMSN_3$ and formation of $N(TMS)(Bpin)_2$ after 12 hours in C_6D_6 at 100 °C (Scheme 5).

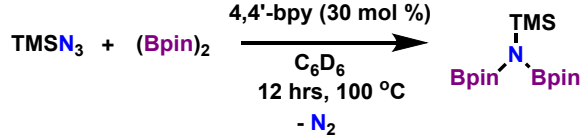

Scheme 5. Organocatalytic borylation of Me_3SiN_3 to form an amine

This provides a facile synthesis of mixed boryl/silyl amines, which have previously been synthesized via $(TMS)_3N$ and boryl halides.[29]

The silyl transfer reagent **2** reacts with tetrazines at room temperature to give the reduced, silylated tetrazines.[30] With this in mind, we sought analogous reactivity with $(Bpin)_2$ and catalytic 4,4'-bpy. Reaction of Ph_2Tz with $(Bpin)_2$ and 30 mol % 4,4'-bpy results in quantitative conversion to the reduced tetrazine after 12 hours in d_8-THF at 80 °C (Scheme 6).

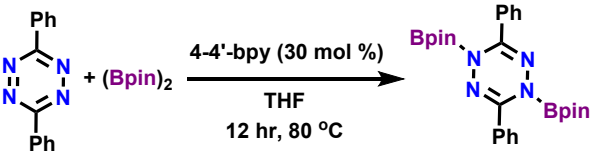

Scheme 6. Organocatalytic borylation of Ph_2Tz

Interestingly, despite tetrazines having more positive reduction potentials than pyrazines, Ph_2Tz and $(Bpin)_2$ do not react without 4,4'-bpy acting as a Bpin shuttle, which can be explained by Suginome's proposed mechanism for the borylation of pyrazine with $(Bpin)_2$.[9, 31]

RNO_x Deoxygenation

We wanted to further exploit the affinity of boryl groups for heteroatoms, and thus sought borylation and reductive removal of oxygen. Deoxygenation of nitrobenzene with bis-silyl 4,4'-bipyridine has been studied in some detail, with Mashima reporting complete deoxygenation of $PhNO_2$ with excess $(TMS)_2$bpy to give $PhN(TMS)_2$, as well as single deoxygenation followed by N/O silylation.[32] Due to the silylated 4,4'-bipyridine being more effective than silylated pyrazines for deoxygenation of $PhNO_2$, we also sought stoichiometric $PhNO_2$ deoxygenation with the reduced 4,4'-bipyridine analogue **3**, which was synthesized following the established procedure.[11] The addition of 2.5 equivalents of **3** to $PhNO_2$ at 25 °C in C_6D_6 affords a yellow solution, and despite the poor solubility of **3**, full consumption of $PhNO_2$ is complete within 30 minutes. The ^{1}H NMR spectrum (Fig S7) indicates complete conversion to a single new product, as judged

by the three aromatic resonances of appropriate intensities. The methyl region contains three signals with intensities of 1:1:2, corresponding to the N/O borylated product (Scheme 7) as well as the boryl ether, $(Bpin)_2O$. While this manuscript was in revision, a paper was published showing this same result.[33]

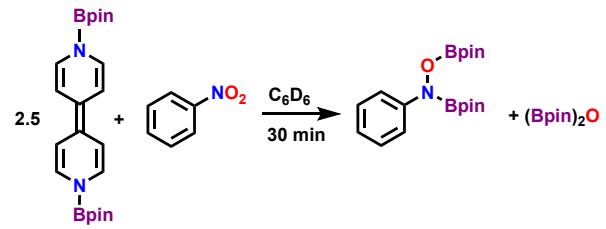

Scheme 7. Partial deoxygenation of $PhNO_2$ using **3**

DFT calculations of reaction thermodynamics (see SI) show consistently that silylation is uniformly more exergonic than borylation by 20-26 Kcal/mol, and that the 4,4'-bipyridine reagent $(Bpin)_2Bpy$ is uniformly more powerful than $(Bpin)_2Pz$ by ~9 Kcal/mol, which is consistent with Mashima's and Suginome's experimental observations. Despite the thermodynamic favorability of silylation, borylation proceeds in several instances where silylation does not (*vide supra*), which supports our hypothesis of lower kinetic barriers using borylated heterocycles compared to their silylated counterparts. The reactivity of **3** with $PhNO_2$ shows that reduced borylated heterocycles are capable of deoxygenation; therefore, we turned our attention to reductive deoxygenation of a coordinated metal nitrate.

Nitrate Deoxygenation

We targeted reduction of pentavalent nitrogen in NO_3^- in order to test how many deoxygenation steps are possible, with anticipated products being NO_2^-, NO^q (q = -1, 0, +1), or even N^{3-}. We chose $Fe(NO_3)_2$ as our target unit, to add the alternatives of reducing one nitrate multiple times vs. both nitrates fewer times, along with the variable of a redox active metal. Iron was chosen with the anticipation of DNICs (dinitrosyl iron complexes), $L_nFe(NO)_2$, being a thermodynamic sink, given the number of such compounds, as well as their selection by evolution for biological applications.[34] An α-diimine ancillary ligand was chosen for its ability to incorporate steric bulk in N substituents, more than for its redox non-innocence.[35, 36]

Reaction of $FeCl_2$ in THF with DIM (DIM = N,N'-bis(2,4,6-trimethylphenyl)-1,4-diaza-2,3-dimethyl-1,3-butadiene) (1:1 mole ratio) in THF occurs with immediate color change to dark blue. Workup yields a violet solid whose ^1H NMR chemical shifts (Fig S8) and intensities are indicative of a paramagnetic species with C_{2v} symmetry (Scheme 8), consistent with formation of $(DIM)FeCl_2$.

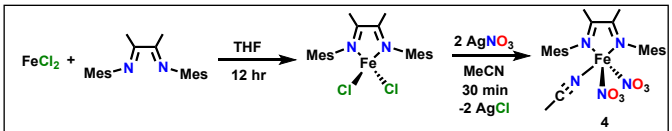

Scheme 8. Synthesis of **4** from $(DIM)FeCl_2$

$AgNO_3$ in CD_3CN was added (2:1 mole ratio) to $(DIM)FeCl_2$, and upon addition, there was a slight color change to a deeper purple, as well as the formation of a white precipitate. A ^1H NMR spectrum (Fig S9) of the product solution reveals complete consumption of $(DIM)FeCl_2$ and conversion to a single paramagnetic product with chemical shifts and intensities indicative of C_{2v} symmetry. An IR spectrum of the product (Fig S12) shows strong absorptions, absent in $(DIM)FeCl_2$, at 1506 and 1270 cm^{-1}, attributed to nitrate. A single crystal suitable for X-ray diffraction was grown by layering ether on a concentrated MeCN solution of the product **4**. The molecular structure obtained (Fig 3) shows bidentate diimine ligand and two nitrates, together with one coordinated acetonitrile. Additional acetonitrile fills the packing voids. Each nitrate coordinates iron in a bidentate fashion, but with one FeO distance longer than the other by ~0.14 Å. The NO distances become longer as the O is closer to Fe, with the terminal NO shortest of all, at 1.22 Å. This species changes color from purple in acetonitrile to yellow in THF, suggesting that the acetonitrile ligand is labile towards replacement by other nucleophiles.

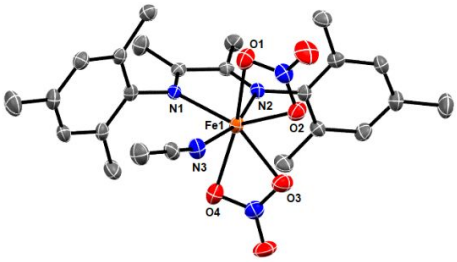

Fig 3. Molecular structure of **4** showing selected atom labelling. Ellipsoids are plotted at the 50% probability level. Unlabelled atoms are carbons. Hydrogen atoms are omitted for clarity. Selected structural parameters (Å): Fe1-O2, 2.179(2); Fe1-O1, 2.321(2); Fe1-O4, 2.362(2); Fe1-O3, 2.183(2); Fe1-N1, 2.193(2); Fe1-N2, 2.163(2); Fe1-N3, 2.168(3).

Deoxygenation of nitrate was next attempted (Scheme 9) by reaction of $(DIM)Fe(NO_3)_2(MeCN)$ with $(Bpin)_2Pz$ at a 1:4 mole ratio in d_8-THF, giving a color change from light purple to dark purple; all $(DIM)Fe(NO_3)_2(MeCN)$ was consumed after 36 hours of mixing at room temperature, as judged by ^1H NMR. The ^1H NMR spectrum (Fig S10) of the resulting solution shows a single diamagnetic product, with ligand resonances consistent with C_{2v} symmetry and with appropriate intensities. Also seen at appropriate intensities for the balanced reaction are signals of pyrazine and $(Bpin)_2O$. Because of the simplicity of its ^1H NMR spectrum, the $O(Bpin)_2$ can be a valuable asset for establishing reaction stoichiometry, as well as time evolution of a reaction and detection of intermediates. The IR spectrum of this solution (Fig S13) shows strong absorptions at 1697 and 1645 cm^{-1}, consistent with other observed four coordinate DNICs.[37] Compared to free NO at 1843 cm^{-1},[38] these values show strong back donation in the product.

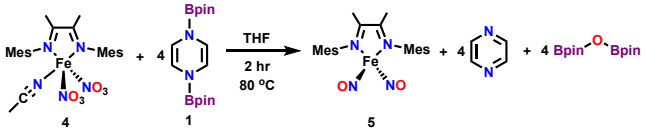

Scheme 9. Synthesis of **5** from **4** using four equivalents of **1**

The spectroscopic properties are confirmed by single crystal X-ray diffraction (Fig 4) as containing the bidentate diimine ligand and two linear nitrosyls, in a distorted tetrahedral structure, **5**. The Fe/N(diimine) distances here are shorter by 0.15 Å, than in the paramagnetic nitrate complex, consistent with occupancy of antibonding Fe/N orbitals in $(DIM)Fe(NO_3)_2(MeCN)$. In both Fe/DIM compounds, the DIM C-N distances, ~1.28 Å, are shorter than the

diazabutadiene C-C distances, 1.48–1.51 Å, indicating that this ligand is neutral, not reduced by the metal.[39-41]

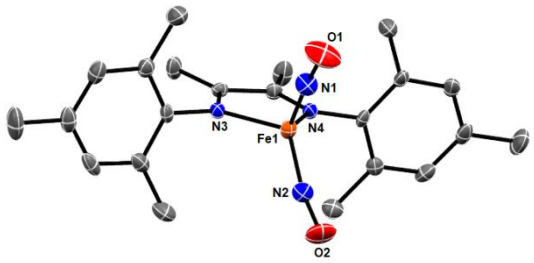

Fig 4. Molecular structure of **5** showing selected atom labelling. Ellipsoids are plotted at the 50% probability level. Unlabelled atoms are carbons. Hydrogen atoms are omitted for clarity. Selected structural parameters (Å): Fe1-N3, 2.038(2); Fe1-N4, 2.014(3); Fe1-N2, 1.654(3); Fe1-N1, 1.648(3); O2-N2, 1.201(3); N1-O1, 1.192(3); O2-N2-Fe1, 167.6(3); O1-N1-Fe1, 174.3(3).

The conversion of **4** to **5** is complete in 2 hours at 80 °C in d_8-THF, and this is the first example of DNIC formation from an iron bis-nitrate starting material, although deoxygenation of nitrite to NO using PPh_3 has been shown,[42] as well as ligand based reduction of a nitrate salt to form a DNIC, assisted by a pendant ligand ammonium proton.[17]

The overall redox transformation accomplished in Equation 1 is complicated by the redox non-innocence of the nitrosyl ligands. Despite having nearly linear nitrosyl ligands (here ∠FeNO is 174.29° and 167.58°), previous work has best described $\{Fe(NO)_2\}^{10}$ complexes as $\{Fe^{II}(NO^-)_2\}$, where the S = 2 iron center is antiferromagnetically coupled to the two NO^- triplets.[34, 43, 44] This antiferromagnetic coupling then contributes to the nitrosyl linearity, rehybridizing the sp^2 nitrogen (expected for NO^- singlet) to have more sp character. The redox innocence of the DIM ligand in **5** suggests that the nitrosyl ligands are more oxidizing than DIM. With this electronic structure picture in mind, all eight electrons delivered in this process go to the nitrogen oxyanion ligand, taking pentavalent nitrogen to monovalent nitrogen, a successful four electron reduction of each nitrate.

$$Fe^{2+} + 2\ NO_3^- + 8e^- \longrightarrow Fe(NO)_2 + 4\ O^{2-} \qquad \text{Eq. 1}$$

We evaluated Mössbauer spectroscopy of both **4** and **5** for insight into electronic structure and comparison to known analogues. The Mössbauer spectrum of $(DIM)Fe(NO_3)_2(MeCN)$, **4**, shows (Fig. 5) two doublets of equal intensity, indicating two (very similar) iron environments with isomer shifts of 1.20 and 1.14 mm s^{-1}, and quadrupole splittings of 3.04 and 2.15 mm s^{-1}. Since the crystal structure has only one molecule in the asymmetric unit, we attribute this feature to either the presence of two different solvation isomers (different MeCN content, consistent with slight color change on grinding sample for MB measurement) or species differing in the quasi bidentate character of nitrate already established in the crystal structure determination. The Mössbauer parameters are consistent with high spin Fe(II) for both species with a high coordination number. The large isomer shifts are comparable to other 7-coordinate species reported,[45, 46] supporting the observed denticity of nitrate in the crystal structure, and ^{1}H NMR assay of the Mössbauer sample after analysis is consistent with **4**, ruling out one of the doublets being due to impurities or oxidation product. The Mössbauer spectrum of **5** (Fig. 5) shows a doublet with an isomer shift of 0.25 and quadrupole splitting of 0.65, similar to other reported neutral DNICs.[47, 48] $\{Fe(NO)_2\}^{10}$ complexes tend to have surprisingly small isomer shifts due to a high degree of π-backdonation into the nitrosyl ligands, which is supported by the low NO stretching frequencies of **5**.[44, 47, 49]

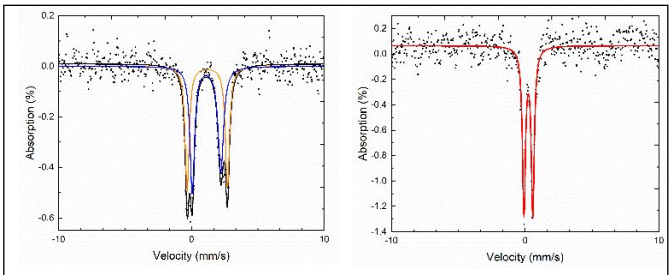

Fig 5. Mossbauer spectra of (a) **4** and (b) **5** at 77 K.

The redox properties of DNICs have been well studied, and DNICs can be classified as either the S = ½ $\{Fe(NO)_2\}^9$ or the diamagnetic $\{Fe(NO)_2\}^{10}$ using Enemark-Feltham notation.[50] With **5** being of the type $\{Fe(NO)_2\}^{10}$, we were interested in oxidation to form $[(DIM)Fe(NO)_2]^+$. Given that DIM is in an oxidized state, any oxidation is predicted to occur within the $Fe(NO)_2$ unit. The reaction of **5** with equimolar $[FeCp_2](OTf)$ results in a color change from dark purple to maroon, and within 15 minutes in d_8-THF all ^{1}H NMR signals for **5** were gone. A solid state IR of the oxidized $\{Fe(NO)_2\}^9$ product (Fig S14) shows strong N-O stretches at 1782 and 1705 cm^{-1}, shifted higher by 85 and 60 cm^{-1} compared to **5**, which can be attributed to decreased electron density at the iron center and thus less backdonation to the nitrosyl ligands, consistent with other $\{Fe(NO)_2\}^9$ complexes.[17, 37, 47, 48, 51, 52] Room temperature EPR spectroscopy of the oxidized product gives a 13 line pattern with a g value of 2.023, consistent with an iron based radical (Fig. 6), explained by coupling to two inequivalent pairs of nitrogens, two nitrosyl nitrogens and two DIM nitrogens, with coupling constants of a_{N1} = 3.4 G and a_{N2} = 5.4 G, similar to coupling constants observed for other DNICs with ancillary N donors (see supporting information for simulation).[42, 53-55]

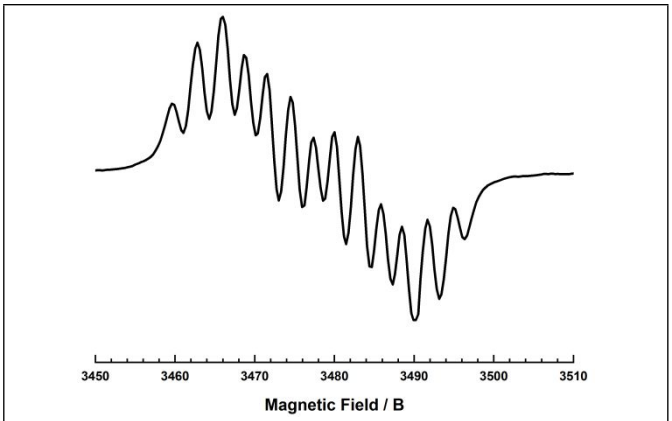

Fig 6. EPR spectrum of $[DIMFe(NO)_2]^+$ in THF with g_{av} = 2.023 (a_{N1} = 3.4 G; a_{N2} = 5.4 G) at 298 K

Computations were done at the TPSSH/def2TZVP level of theory to gain insight into the electronic structure of the oxidized species; the TPSSH functional has been shown to best represent the electronic structure of DNICs.[44] The HOMO of **5** (Fig. 7a) is comprised of an iron d orbital backdonating into the nitrosyl ligands, as well as a small amount of DIM nitrogen character. Thus, oxidation should leave a single electron in this orbital allowing it to couple to each of the nitrogens coordinated to iron. The spin density plot (Fig. 7b) of

$[(DIM)Fe(NO)_2]^+$ corroborates the coupling to all four nitrogens, showing spin density on iron, the nitrosyl ligands, and the DIM nitrogens. Furthermore, the unrestricted corresponding orbital diagram (SI Figures S16-17) shows the unpaired spin to lie primarily in d_{x2-y2}, with spin density on all four nitrogens. The calculated NO stretching frequencies of the neutral and cation are within 50 cm^{-1} of those observed, an error consistent with that observed previously, where the conclusion was that this unit is highly covalent, and integral oxidation states and a single electron configuration inadequately describes reality.[44]

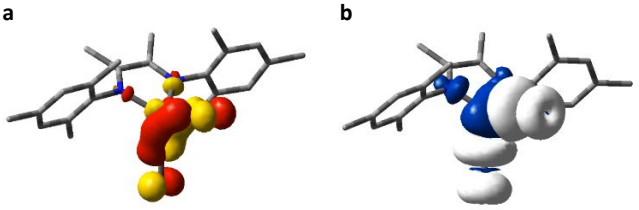

Fig 7. a) HOMO of **5** (isovalue 0.05) **b**) Spin density plot of $[(DIM)Fe(NO)_2]^+$ (isovalue 0.002)

The fact that the reduced nitrosyl nitrogen is attached to a redox active metal adds to the value of this conversion, particularly for subsequent functionalization of that reduced nitrogen. For example, we expect increased electrophilicity on the nitrosyl nitrogens owing to a more oxidized metal center, and thus less backdonation; consequently, nucleophilic attack on nitrogen in the DNIC cation should be enhanced, with possible products of RNO, R_2NNO and RSNO.[56-59] In addition it may be possible to use the capture of two nitrogens at a single metal center in either the neutral or the cation as a useful organizational step in making an N/N bond from the reduced species.[60] Given the spin density on both nitrogens in Figure 7b, radical coupling could be favored. Several nitrogen reductases form N_2O from nitrosyl ligands attached to iron or copper, and a recent example of a DNIC converting nitric oxide to N_2O has been reported, but the mechanism is bimolecular in iron.[61-63] Hayton has shown bimolecular coupling of two nickel nitrosyls to form N_2O via an isolable hyponitrite intermediate.[64, 65] With our interest in the potential for N=N bond formation from a DNIC, computations were done on the isomeric *hyponitrite* structure, with a starting geometry of tetrahedral Fe(II), $DIMFe(\kappa^2\text{-}ON{=}NO)$. Of exceptional importance, this S = 2 hyponitrite structure optimizes to a square planar complex, and is 4.6 kcal/mol more stable than the DNIC isomer. What remains for the future is to find excitation conditions which can cause the major rearrangements needed to break two Fe-N(nitrosyl) bonds in preparation for forming the NN bond of hyponitrite, but the thermodynamic viability of such isomerization of DNICs demands inquiry. Furthermore, given the demonstrated ability of $(DIM)Fe(NO)_2$ to also undergo one electron reduction,[66] this sets three oxidation levels, $\{Fe(NO)_2\}^9$, $\{Fe(NO)_2\}^{10}$, and $\{Fe(NO)_2\}^{10}$-reduced, available for future manipulation of nitrogen oxidation state, starting from either electron rich (DNIC anion) or electron poor (DNIC cation) surrounding of monovalent nitrosyl nitrogen.

Conclusions

Overall, these results show the broad potential of using these several Bpin transfer reagents incorporating polar B-N bonds for reduction of double bonds between N and other heteroatoms. Possible extensions of this method to deoxygenation of other oxyanions such as carbonate, phosphate, perchlorate, or sulfate remain to be explored, as well as deoxygenation of small molecules, including CO_2 and CO. Nonetheless, these reagents provide a new capability for N=N bond reduction and N-deoxygenation generally, beyond the already powerful bis-silyl pyrazine/bipyridine reductants.

Conflicts of interest

The authors declare no conflict of interest.

Acknowledgements

This work was supported by the Indiana University Office of Vice President for Research and the National Science Foundation, Chemical Synthesis Program (SYN), by grant CHE-1362127. We thank Jorge Martinez for the MB measurements, and I. J. Huerfano for the synthesis of the DIM ligand.

Notes and references

1. K. Yang, F. Zhou, Z. Kuang, G. Gao, T. G. Driver and Q. Song, *Org. Lett.*, 2016, **18**, 4088-4091.
2. Y. Guindon, J. G. Atkinson and H. E. Morton, *J. Org. Chem.*, 1984, **49**, 4538-4540.
3. A. Volkov, K. P. J. Gustafson, C.-W. Tai, O. Verho, J.-E. Bäckvall and H. Adolfsson, *Angew. Chem. Int. Ed.*, 2015, **54**, 5122-5126.
4. H. Sajiki, A. Mori, T. Mizusaki, T. Ikawa, T. Maegawa and K. Hirota, *Org. Lett.*, 2006, **8**, 987-990.
5. A. B. Cuenca, R. Shishido, H. Ito and E. Fernández, *Chem. Soc. Rev.*, 2017, **46**, 415-430.
6. E. C. Neeve, S. J. Geier, I. A. I. Mkhalid, S. A. Westcott and T. B. Marder, *Chem. Rev.*, 2016, **116**, 9091-9161.
7. J. Seo, A. C. Cabelof, C.-H. Chen and K. G. Caulton, *Chem. Sci.*, 2019, **10**, 475-479.
8. H. Tsurugi and K. Mashima, *Acc. Chem. Res.*, 2019, **52**, 769-779.
9. K. Oshima, T. Ohmura and M. Suginome, *Chem. Commun.*, 2012, **48**, 8571-8573.
10. W. Kaim, *J. Am. Chem. Soc.*, 1983, **105**, 707-713.
11. T. Ohmura, Y. Morimasa and M. Suginome, *J. Am. Chem. Soc.*, 2015, **137**, 2852-2855.
12. T. Ohmura, Y. Morimasa and M. Suginome, *Chem. Eur. J.*, 2017, **46**, 1793-1796.
13. R. J. Diaz and R. Rosenberg, *Science*, 2008, **321**, 926.
14. S. Xu, D. C. Ashley, H.-Y. Kwon, G. R. Ware, C.-H. Chen, Y. Losovyj, X. Gao, E. Jakubikova and Jeremy M. Smith, *Chem. Sci.*, 2018, **9**, 4950-4958.
15. C. L. Ford, Y. J. Park, E. M. Matson, Z. Gordon and A. R. Fout, *Science*, 2016, **354**, 741.
16. E. M. Matson, Y. J. Park and A. R. Fout, *J. Am. Chem. Soc.*, 2014, **136**, 17398-17401.
17. M. Delgado and J. D. Gilbertson, *Chem. Commun.*, 2017, **53**, 11249-11252.
18. Y. M. Kwon, M. Delgado, L. N. Zakharov, T. Seda and J. D. Gilbertson, *Chem. Commun.*, 2016, **52**, 11016-11019.
19. C. Uyeda and J. C. Peters, *J. Am. Chem. Soc.*, 2013, **135**, 12023-12031.
20. Y. Liu and J. Wang, *Sci. Total. Environ.*, 2019, **671**, 388-403.
21. K. T. Burns, W. R. Marks, P. M. Cheung, T. Seda, L. N. Zakharov and J. D. Gilbertson, *Inorg. Chem.*, 2018, **57**, 9601-9610.
22. Y.-L. Chang, Y.-F. Lin, W.-J. Chuang, C.-L. Kao, M. Narwane, H.-Y. Chen, M. Y. Chiang and S. C. N. Hsu, *Dalton Trans.*, 2018, **47**, 5335-5341.

23. C. M. Moore and N. K. Szymczak, *Chem. Sci.*, 2015, **6**, 3373-3377.
24. B. C. Sanders, S. M. Hassan and T. C. Harrop, *J. Am. Chem. Soc.*, 2014, **136**, 10230-10233.
25. J. Gwak, S. Ahn, M.-H. Baik and Y. Lee, *Chem. Sci.*, 2019, **10**, 4767-4774.
26. S. Park and S. Chang, *Angew. Chem. Int. Ed.*, 2017, **56**, 7720-7738.
27. M. B. Ansell, G. E. Kostakis, H. Braunschweig, O. Navarro and J. Spencer, *Adv. Synth. Catal.*, 2016, **358**, 3765-3769.
28. J. J. Kiernicki, R. F. Higgins, S. J. Kraft, M. Zeller, M. P. Shores and S. C. Bart, *Inorg. Chem.*, 2016, **55**, 11854-11866.
29. J. F. Janik, C. K. Narula, E. G. Gulliver, E. N. Duesler and R. T. Paine, *Inorg. Chem.*, 1988, **27**, 1222-1227.
30. D. M. Beagan, I. J. Huerfano, A. V. Polezhaev and K. G. Caulton, *Chem. Eur. J.*, 2019, **25**, 8105-8111.
31. S. J. Geier, C. M. Vogels, N. R. Mellonie, E. N. Daley, A. Decken, S. Doherty and S. A. Westcott, 2017, **23**, 14485-14499.
32. A. Bhattacharjee, H. Hosoya, H. Ikeda, K. Nishi, H. Tsurugi and K. Mashima, *Chem. Eur. J.*, 2018, **24**, 11278-11282.
33. H. Hosoya, L. C. Misal Castro, I. Sultan, Y. Nakajima, T. Ohmura, K. Sato, H. Tsurugi, M. Suginome and K. Mashima, *Org. Lett.*, 2019, DOI: 10.1021/acs.orglett.9b03419.
34. M.-L. Tsai, C.-C. Tsou and W.-F. Liaw, *Acc. Chem. Res.*, 2015, **48**, 1184-1193.
35. L. Gonsalvi, J. A. Gaunt, H. Adams, A. Castro, G. J. Sunley and A. Haynes, *Organometallics*, 2003, **22**, 1047-1054.
36. S. C. Bart, E. J. Hawrelak, A. K. Schmisseur, E. Lobkovsky and P. J. Chirik, *Organometallics*, 2004, **23**, 237-246.
37. C.-H. Ke, C.-H. Chen, M.-L. Tsai, H.-C. Wang, F.-T. Tsai, Y.-W. Chiang, W.-C. Shih, D. S. Bohle and W.-F. Liaw, *J. Am. Chem. Soc.*, 2017, **139**, 67-70.
38. K. Nakamoto, *Infrared Spectra of Inorganic and Coordination Compounds*, 1963.
39. T. Schaub and U. Radius, *Anorg. Allg. Chem.,* 2006, **632**, 807-813.
40. S. J. Kraft, U. J. Williams, S. R. Daly, E. J. Schelter, S. A. Kozimor, K. S. Boland, J. M. Kikkawa, W. P. Forrest, C. N. Christensen, D. E. Schwarz, P. E. Fanwick, D. L. Clark, S. D. Conradson and S. C. Bart, *Inorg. Chem.*, 2011, **50**, 9838-9848.
41. E. K. Cope-Eatough, F. S. Mair, R. G. Pritchard, J. E. Warren and R. J. Woods, *Polyhedron*, 2003, **22**, 1447-1454.
42. F.-T. Tsai, P.-L. Chen and W.-F. Liaw, *J. Am. Chem. Soc.*, 2010, **132**, 5290-5299.
43. J. L. Hess, C.-H. Hsieh, S. M. Brothers, M. B. Hall and M. Y. Darensbourg, *J. Am. Chem. Soc.*, 2011, **133**, 20426-20434.
44. S. Ye and F. Neese, *J. Am. Chem. Soc.*, 2010, **132**, 3646-3647.
45. A. K. Bar, C. Pichon, N. Gogoi, C. Duhayon, S. Ramasesha and J.-P. Sutter, *Chem. Commun.*, 2015, **51**, 3616-3619.
46. H. S. Soo, M. T. Sougrati, F. Grandjean, G. J. Long and C. J. Chang, *Inorg. Chim. Acta*, 2011, **369**, 82-91.
47. A. L. Speelman, B. Zhang, A. Silakov, K. M. Skodje, E. E. Alp, J. Zhao, M. Y. Hu, E. Kim, C. Krebs and N. Lehnert, *Inorg. Chem.*, 2016, **55**, 5485-5501.
48. Z. J. Tonzetich, L. H. Do and S. J. Lippard, *J. Am. Chem. Soc.*, 2009, **131**, 7964-7965.
49. M. Li, D. Bonnet, E. Bill, F. Neese, T. Weyhermüller, N. Blum, D. Sellmann and K. Wieghardt, *Inorg. Chem.*, 2002, **41**, 3444-3456.
50. J. H. Enemark and R. D. Feltham, *Coord. Chem. Rev.*, 1974, **13**, 339-406.
51. P.-H. Liu, F.-T. Tsai, B.-H. Chen, I. J. Hsu, H.-H. Hsieh and W.-F. Liaw, *Dalton Trans.*, 2019, **48**, 6040-6050.
52. C.-Y. Chiang, M. L. Miller, J. H. Reibenspies and M. Y. Darensbourg, *J. Am. Chem. Soc.*, 2004, **126**, 10867-10874.
53. M. W. Foster and J. A. Cowan, *J. Am. Chem. Soc.*, 1999, **121**, 4093-4100.
54. M.-L. Tsai and W.-F. Liaw, *Inorg. Chem.*, 2006, **45**, 6583-6585.
55. W.-C. Shih, T.-T. Lu, L.-B. Yang, F.-T. Tsai, M.-H. Chiang, J.-F. Lee, Y.-W. Chiang and W.-F. Liaw, *J. Inorg. Biochem.*, 2012, **113**, 83-93.
56. A. J. P. Cardenas, R. Abelman and T. H. Warren, *Chem. Commun.*, 2014, **50**, 168-170.
57. M. M. Melzer, S. Mossin, X. Dai, A. M. Bartell, P. Kapoor, K. Meyer and T. H. Warren, *Angew. Chem. Int. Ed.*, 2010, **49**, 904-907.
58. S. Zhang, N. Çelebi-Ölçüm, M. M. Melzer, K. N. Houk and T. H. Warren, *J. Am. Chem. Soc.*, 2013, **135**, 16746-16749.
59. S. Kundu, W. Y. Kim, J. A. Bertke and T. H. Warren, *J. Am. Chem. Soc.*, 2017, **139**, 1045-1048.
60. S. Kundu, P. N. Phu, P. Ghosh, S. A. Kozimor, J. A. Bertke, S. C. E. Stieber and T. H. Warren, *J. Am. Chem. Soc.*, 2019, **141**, 1415-1419.
61. W.-Y. Wu, C.-N. Hsu, C.-H. Hsieh, T.-W. Chiou, M.-L. Tsai, M.-H. Chiang and W.-F. Liaw, *Inorg. Chem.*, 2019, DOI: 10.1021/acs.inorgchem.9b01635.
62. A. B. McQuarters, N. E. Wirgau and N. Lehnert, *Curr. Opin. Chem. Biol.*, 2014, **19**, 82-89.
63. A. C. Merkle and N. Lehnert, *Dalton Trans.*, 2012, **41**, 3355-3368.
64. A. M. Wright, G. Wu and T. W. Hayton, *J. Am. Chem. Soc.*, 2012, **134**, 9930-9933.
65. A. M. Wright, H. T. Zaman, G. Wu and T. W. Hayton, *Inorg. Chem.*, 2014, **53**, 3108-3116.
66. C.-H. Ke, W.-C. Shih, F.-T. Tsai, M.-L. Tsai, W.-M. Ching, H.-H. Hsieh and W.-F. Liaw, *Inorg. Chem.*, 2018, **57**, 14715-14726.

Reductive Borylation

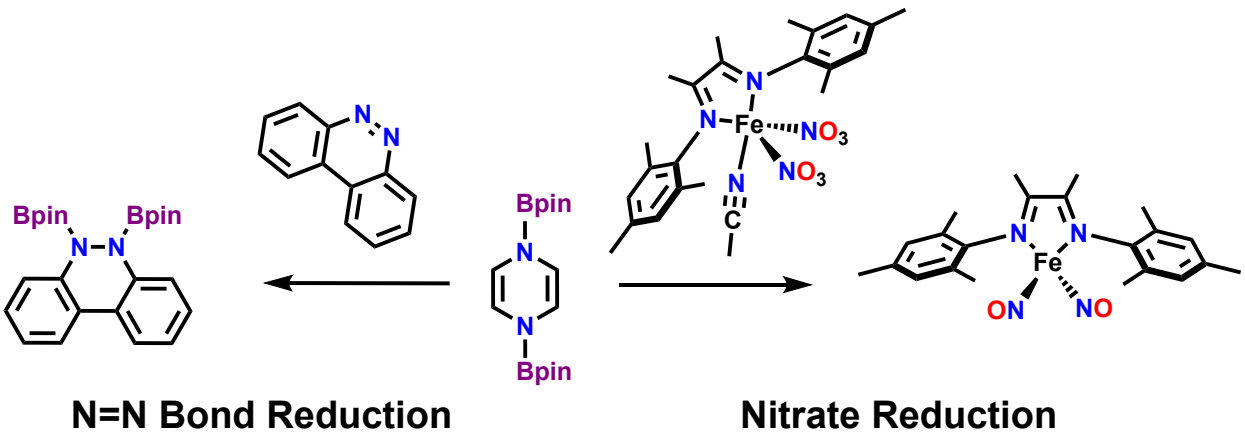

N=N Bond Reduction **Nitrate Reduction**

Borylated heterocycles are shown to be potent reductants towards organic substrates, as well as capable of nitrate deoxygenation,